

Original Article

Image quality characteristics of myocardial perfusion SPECT imaging using state-of-the-art commercial software algorithms: evaluation of 10 reconstruction methods

Taher Hosny¹, Magdy M Khalil², Abdo A Elfiky¹, Wael M Elshemey¹

¹Department of Biophysics, Faculty Science, Cairo University, Cairo, Egypt; ²Department of Physics, Faculty of Science, Helwan University, Cairo, Egypt

Received December 20, 2019; Accepted October 2, 2020; Epub December 15, 2020; Published December 30, 2020

Abstract: Myocardial perfusion imaging (MPI) is widely used as standard of care in patients with coronary artery disease. The availability of hybrid SPECT/CT imaging system and associated advanced reconstruction algorithms serve to improve diagnostic accuracy and enhances image quality of MPI. The aim of this work was to evaluate the relative performance of iterative reconstruction algorithms correcting for different combinations of image degrading factors versus filtered back projection on the quality of myocardial perfusion SPECT imaging. A standard cardiac phantom containing myocardial defects of different sizes and compositions was used to simulate myocardial perfusion SPECT/CT clinical studies. A clinically relevant activity was determined to avoid discordance with real data acquisition. Acquisition parameters including time per projection, angular rotation increment, and iterative reconstruction number of iterations and subsets were varied. The reconstruction was carried out applying different algorithms including 10 variants of analytical (e.g FBP) and iterative reconstructions with and without resolution recovery. Typical figures of merit were used to evaluate the image quality of MPI reconstructed with ten different reconstruction methods. OSEM-RR showed remarkable improvement of image quality of MPI in terms of SNR, CNR and defect contrast percentage compared to FBP algorithm. Full correction scheme IR-RR (i.e. IRACSCRR) provides clinically acceptable image quality of MPI compared to FBP.

Keywords: Myocardial perfusion, resolution recovery, attenuation correction, scatter correction, iterative reconstruction

Introduction

Myocardial perfusion imaging (MPI) using single photon computed tomography (SPECT) is well established noninvasive imaging technique and widely used to evaluate patients with known or suspected coronary artery disease (CAD) [1]. Several studies have shown the strong diagnostic and prognostic value of SPECT MPI [2-4]. Gated SPECT of MPI can provide accurate diagnosis about tracer distribution over myocardial walls as well as left ventricular function in one diagnostic procedure. New hardware and software developments in addition to hybrid imaging including SPECT and multi-slice CT (SPECT/CT) have made a significant improvement to image quality and diagnostic accuracy [4, 5].

Although there are several techniques for creating a patient specific SPECT reconstructions attenuation maps (e.g. ¹⁵³Gd-100 keV transmission source), the x-ray tube in hybrid SPECT/CT offers a unique opportunity in terms of generating low noise attenuation maps and speed as well as scan reproducibility. The implementation of SPECT/CT scanners in routine nuclear medicine studies allows the attenuation correction from all tissue types (e.g., soft, bone, lung) with remarkable advantages over other conventional systems. It resolves the cross-talk between SPECT radionuclides and the radioactive transmission source creating high quality attenuation map and reduce total scan time [7-9].

Scattered photons within patient body or collimator are also potential sources of image deg-

radation. About 30-50% of total counts within the photo peak window are scattered photons depending on radionuclide photo peak energy window and the body region to be imaged [10]. This fraction of scattered photons degrades image quality in terms of contrast and quantification accuracy [11]. Scatter correction has been implemented through different approaches including dual energy window (DEW), triple energy window (TEW) and convolution subtraction method [12].

Collimator detector response (CDR) as an image degrading factor has been the subject of intensive research and development to improve SPECT reconstructed image resolution and resolve the partial volume phenomenon. Compensation for CDR depends on many factors such as septal penetration, septal scattering, geometric CDR and detector intrinsic resolution [13]. Myocardial images corrected for CDR further improves quantitative accuracy, spatial resolution and contrast but associated with slight increase in noise [14].

New reconstruction methods have been proposed to overcome the drawbacks associated with analytical methods. Iterative reconstruction (IR) has been the alternative method most commonly implemented in cardiac reconstruction as well as other SPECT studies. IR such as ordered subset expectation maximization (OSEM) and/or maximum likelihood expectation-maximization (MLEM) has the ability to reduce the noise level accompanied with the iterative process by using noise suppression methods controlled by post filtering [15].

Several studies have shown the potential of iterative algorithm accompanied with attenuation, scatter and resolution recovery to improve overall diagnostic accuracy, quantification analysis, localization of perfusion defects as well as detection of CAD [13, 16].

Now commercially available OSEM incorporates resolution recovery, attenuation and scatter corrections in MPI SPECT. Those software packages are namely Astonish (Philips Healthcare, Eindhoven, The Netherlands), Evolution for Cardiac, EfC (GE Medical Systems, Waukesha, WI, USA), Flash3D (Siemens Medical Solutions), and wide-beam reconstruction (WBR) [UltraSPECT, Ltd] [5, 17, 18].

While the cardiac iterative reconstruction algorithm Myovation Evolution, (GE Health Care) has become commercially available for routine reconstruction of MPI, it is of great importance to be extensively evaluate it on a technical/clinical level before full implementation in a given clinic. Myovation Evolution is an OSEM algorithm that includes compensation for attenuation, scatter and CDR. The primary aim of the current study was to evaluate the impact of OSEM reconstruction with and without the various corrections in comparison to conventional filtered back projection (FBP). The secondary aim was to figure out the best combination of acquisition and iterative reconstruction parameters (numbers of subsets and iterations, post-filter) that optimize myocardial perfusion image quality.

Materials and methods

A standard cardiac insert with 110 ml myocardium volume and wall thickness of 10 mm was used. Two solid defects, one transmural and one non-transmural, were used as perfusion defects the former was located in mid anterior wall ($45^\circ \times 1.5$ cm), and the latter was inserted at the basal inferior wall ($60^\circ \times 2$ cm, with 5 mm wall thickness). The cardiac insert was placed inside a cylindrical Jaszczak phantom 6000 ml in volume. A clinically relevant activity (i.e. ^{99m}Tc) was injected into the myocardium with a concentration of 8 $\mu\text{Ci/ml}$, simulating myocardium perfusion rest study, while for background the activity concentration was about 2 $\mu\text{Ci/ml}$. The activity concentration was estimated from ten random patients who undergone routine myocardial perfusion SPECT examinations, correlating the injected activity to system sensitivity. A decay factor of 1.12 (one hour post injection) and approximately 30% patient attenuation were employed. The GE Discovery NM670 SPECT/CT system loaded with LEHR collimator (Health Care US) was used for data acquisition.

Acquisition protocol

A manufacturer standard acquisition protocol for cardiac imaging, namely Efc, was selected. SPECT MPI was carried out using L-mode detector geometry. SPECT projection views from right anterior oblique to left posterior oblique were acquired over a total angular rotation of 180° at an increment of 3° rotation employing acqui-

sition matrix of 64×64 with a pixel size of 6.79 mm. To investigate the impact of the acquisition time and count statistics on image quality, four sequential SPECT scans were acquired with four different times per projection including (5, 10, 15 and 20 sec) bearing in mind that 20 sec/projection is the standard acquisition time. Radioactive decay was carefully corrected to compensate for time lapse from one sequential acquisition to another.

Furthermore, four consecutive SPECT scans were acquired with total arc of 180° and an increment of 2° , 3° , 6° and 9° per rotation (i.e. 90, 60, 30, 20 projections respectively) where 60 is the standard number of projections. To ensure concordance of results, other acquisition parameters were maintained fixed, such as a $140 \text{ keV} \pm 10\%$ photo peak energy window, a $120 \text{ keV} \pm 5\%$ scatter window and 64×64 pixels matrix. Only one attenuation CT scan was acquired covering the whole phantom length immediately after the emission scans were completed. The CT acquisition was carried out using helical scan mode with a tube voltage of 120 kV and current of 20 mA. After data acquisition, all files were sent to a common processing and reconstruction workstation provided by the system manufacturer (Xeleris version 3.05, GE Health Care).

Image reconstruction

FBP, OSEM and OSEM-RR with different corrections of image degrading factors were used. A number of different acquisition and reconstruction parameters that could potentially influence image quality in MPI were also investigated including number of projections, total acquisition time, and variable number of iterations and/or subsets using reconstruction algorithms available in the processing workstation. Those algorithms are summarized in **Table 1**.

Acquired data were reconstructed by OSEM IR with and without resolution recovery (RR) providing all corrections as mentioned in **Table 1**. In addition, the following combination of iterations/subsets were applied: 5i/4s, 10i/4s, 20i/4s, 30i/4s, 5i/6s, 10i/6s, 20i/6s, 30i/6s, 5i/12s, 10i/12s, 20i/12, 30i/12s, 5i/15s, 10i/15s, 20i/15s and 30i/15s, for non-corrected NC, attenuation correction AC, scatter correction SC and ACSC reconstructions while maintaining other reconstruction parameters

constant. Furthermore, data of different acquisition times and data of different number of projections were reconstructed iteratively by OSEM algorithm with and without RR applying standard reconstruction parameters given in **Table 1**. Moreover, filtered back projection was applied with and without scatter correction to all acquired data.

Image quality was evaluated based on a number of essential figures of merit such as coefficient of variation (CoV), image uniformity, signal to noise ratio (SNR) and contrast noise ratio (CNR). The former two parameters were measured using maximum count of 60 radial rays of circumferential profiles (ImageJ software, Wayne Rasband, National Institute of Health, USA, version 1.49 m). Thus, an oval ROI of size covering the whole myocardium slice drawn over apical and basal normal slices therefore, the maximum count determined was used for the calculations. The latter two parameters were assessed by drawing a region of interest of half-moon shape of size 8-11 unit area over the lateral wall and neighboring background using available tools in the manufacturer software, see **Figure 1**. Furthermore, percentage defect contrast was evaluated for hypo-perfused segments represented by solid defects. All these physical parameters were evaluated over short axis slices of the reconstructed image.

As mentioned, image uniformity was assessed by 60 radial circumferential profiles drawn over 360° of normally perfused slices of the cardiac phantom. The maximum and minimum counts were determined and slice uniformity was computed using the following formula:

$$\text{Uniformity} = \frac{\text{Max count} - \text{Min coun}}{\text{Max count} + \text{Min count}} * 100$$

Moreover, the coefficient of variation or relative standard deviation of data obtained from circumferential profile was calculated to show the extent of variability over slice uniformity:

$$\text{CV} = \frac{\text{SD}}{\text{mean}} * 100$$

Where *Max count*, *Min count*, *SD* and *mean* are maximum, minimum, standard deviation and mean of myocardial counts of normally perfused three apical slices and two basal slices. The slice selection was carefully made to avoid

SPECT MP image quality with OSEM-RR

Table 1. The methods used in image reconstruction and applied in the present study with description of the reconstruction parameters and combined corrections

Abbreviation	Full name	Implementation
FBP	Filtered back projection	The standard FBP algorithm implemented with Butterworth filter (order of 10 and cut off frequency of 0.3 pixel)
FBPSC	Filtered back projection with scatter correction	The standard FBP algorithm combined with scatter correction. The later was implemented using the acquired scatter window of energy 120 ± 5 keV
IRNC	OSEM reconstruction with no corrections applied	Reconstruction was carried out using 2 iterations and 10 subsets. Data were filtered using Butterworth (order of 10 and cut off frequency of 0.3) and quantitative Ramp filter. Scatter correction was implemented using dual energy window (DEW) of 120 ± 5 keV, CT attenuation map acquired with 120 kV, and 20 mA and helical scan. Scatter and attenuation corrections parameter are applied for IRSC, IRAC and IRACSC.
IRSC	OSEM reconstruction with scatter correction applied	
IRAC	OSEM reconstruction with attenuation correction applied	
IRACSC	OSEM reconstruction with attenuation and scatter corrections applied	
IRNCRR	OSEM reconstruction with resolution recovery correction applied	Reconstruction was performed using 12 iterations and 10 subsets. Data were filtered using Butterworth (order of 10 and cut off frequency of 0.3 pixel) and quantitative Ramp filter. Scatter and attenuation corrections were applied as mentioned above and were maintained for all combination of corrections. Resolution recovery combined with former corrections was implemented through Myovation Evolution software.
IRSCRR	OSEM reconstruction with resolution recovery and scatter corrections applied	
IRACRR	OSEM reconstruction with resolution recovery and attenuation corrections applied	
IRACSCRR	OSEM reconstruction with full corrections applied	

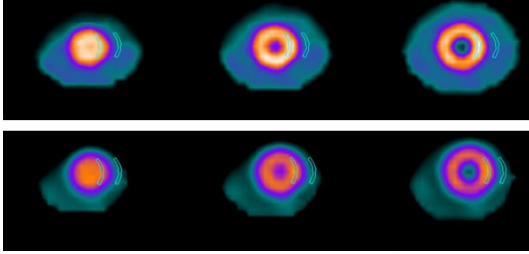


Figure 1. ROI used for CNR and SNR calculations. Half-moon shape of area 8-11 unit area was drawn over lateral wall of apical and basal normal slices using the available tools on Xeleris work station (version 3.05). The figure shows three apical slices reconstructed using IRACSCRR in the upper row and IRAC in the lower row.

Table 2. Acquisition and reconstruction parameters applied in standard and proposed protocols

Parameter	Standard protocol	Proposed protocol
Matrix size	64 × 64	64 × 64
Time/projection	20 sec	5 sec
Number of projection	60	90
Reconstruction algorithm	FBP	OSEM-RR
Iteration/subset	N/A	12iter/10sub
Filter	Butterworth	Butterworth
Cut off frequency/order	0.3/10	0.3/10

apical thinning as well as the most basal myocardial slice. Every effort was also made to align slices minimize slice mismatch.

As nuclear imaging is highly dependent on count statistics and as the main aim of this study was to assess the image quality, it is therefore of particular importance to evaluate signal to noise ratio (SNR) to evaluate myocardial signal level in comparison to the amount of noise in the reconstructed image. Here SNR was calculated as the ratio between mean myocardium counts over background noise:

$$SNR = \frac{Mean\ count_{Myo}}{SD_{Bkg}}$$

Moreover, the contrast to noise ratio was also assessed and was measured using:

$$CNR = \frac{Mean\ count_{Myo} - Mean\ count_{Bkg}}{SQRT(SD_{Myo}^2 - SD_{Bkg}^2)}$$

Where $SQRT(SD_{Myo}^2 - SD_{Bkg}^2)$ is the square root of the myocardial and background squared dif-

ference, and $Mean\ count_{Myo}$ and $Mean\ count_{Bkg}$ are the mean counts of myocardial and background respectively. Percentage defect contrast was calculated to evaluate the defect contrast relative to normal myocardium wall using the following equation:

$$\%Contrast = \frac{Max\ count_{Myo} - Min\ count_{Myo}}{Max\ count_{Myo}} * 100$$

Where $Max\ count_{Myo}$ and $Min\ count_{Myo}$ are maximum and minimum myocardial count respectively obtained from circumferential profile.

After reviewing the whole data set of the above mentioned combination of acquisition/reconstruction parameters, a set of acquisition/reconstruction parameters which showed better results was selected in order to evaluate the validity of results to another set of defects. Moreover, to assess the impact of those proposed parameters on the myocardium perfusion image quality versus standard acquisition/reconstruction parameters. The two defects were of different size and composition than those used in the main data evaluation. One was a solid defect located in the anterior wall ($60^\circ \times 2\text{ cm}$) and the other was cold fillable defect positioned in the inferior wall ($90^\circ \times 2\text{ cm}$, 5.4 ml in volume) of the cardiac insert. Acquisition/reconstruction parameters of standard and proposed protocols are shown in **Table 2**.

Data using the standard and proposed protocol were reconstructed by FBP and OSEM-RR (IRACSCRR) respectively. Reconstructed image was evaluated applying the approach used to evaluate the main data set.

Results

Reconstruction methods

In order to define the baseline of the study, the standard acquisition protocol (20 sec/projection, 3° /rotation) was reconstructed according to the reconstruction parameters mentioned in **Table 1**. Ten reconstruction methods namely FBP, FBPSC, IRNC, IRSC, IRAC, IRACSC, IRNCRR, IRSCRR, IRACRR, IRACSCRR were evaluated. As shown from figures of merit, the performance of the IR algorithm compared to FBP showed continued improvement in terms of CNR, SNR and defect contrast resolution as more corrections were applied (i.e. in the direc-

SPECT MP image quality with OSEM-RR

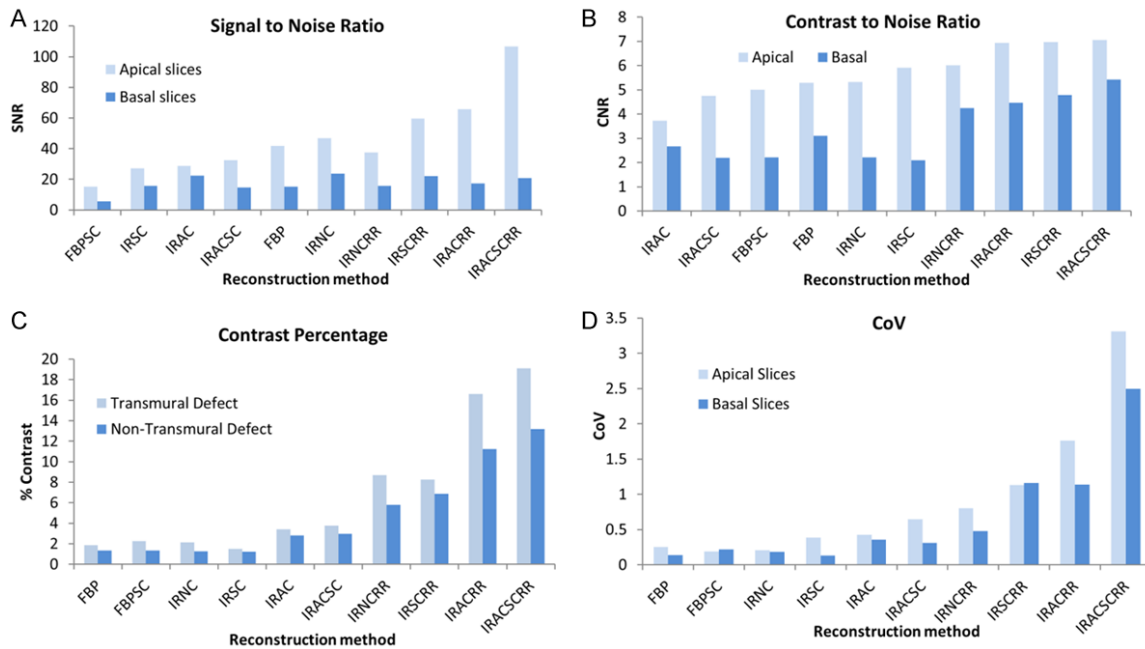


Figure 2. Figures of merit of ten reconstruction algorithm. (A) Signal to Noise Ratio (SNR) of ten reconstruction algorithms for normally perfused apical and basal slices. SNR started to show good performance as RR was applied and in the direction of applying more corrections. (B) Contrast to noise ratio for apical and basal slices, CNR enhancement as RR is applied and reaches its maximum as IR-RR with full corrections are applied. (C) Defect contrast percentage, transmural and non-transmural defects show improvement in the direction of applying more corrections and (D) coefficient of variation shows slight image non-uniformity observed in the direction of adding more corrections.

tion of SC, AC, ACSC and RR) see **Figure 2**. This improvement was calculated as percentage improvement measuring 66%, 77%, 105%, 237%, -16%, -13%, 36%, 254%, -14%, 101%, 88% and 901% for CNR, SNR and defect contrast percentage respectively.

The maximum SNR was obtained with IRAC-SCRR including the apical and basal slices (254% and 110% respectively) when compared to other improvements achieved with other iterative reconstructions combined with different corrections. The defect contrast improvement was noticeable with resolution recovery especially when all corrections were applied (i.e. IRACSCRR). The latter showed an increase of 901% and 709% in comparison to FBP for transmural and non-transmural defects respectively. However, the noise associated with IR was relatively small as revealed by uniformity and CoV analysis. The increase in noise was minimal, as the difference was in the range of 5.0 and 3.3-(at maximum) respectively for uniformity and CoV in comparison to FBP.

To study the impact of IR with different number of iterations/subsets on image quality of MPI

compared to IR-RR and FBP, the standard acquisition was reconstructed applying the reconstruction parameters mentioned in **Table 1**. However, the number of iterations/subsets was changed and IR performed with SC, AC, ACSC and NC for each iteration/subset number. Figures of merit showed that SNR was superior when IR was combined with AC in comparison to IRSC and IRACSC. These results indicated the role of SC in relatively reducing SNR either alone or combined with AC for the wide range of investigated iterations and subset. Nevertheless, comparison of the 4 reconstruction methods with fixed number of iterations and subsets (12i/10s) demonstrated the advantage of using the full correction scheme in significantly improving the SNR in both apical and basal slices, the improvement was 254% and 110% respectively.

Similarly, IRAC was generally superior in terms of CNR when considering all combinations of iterations and subsets. An improvement of 71% and 49% was found in comparison to IRSC (24% and 7%) and IRACSC (52% and 47%) respectively. Those measurements were the best estimate obtained regardless the number

SPECT MP image quality with OSEM-RR

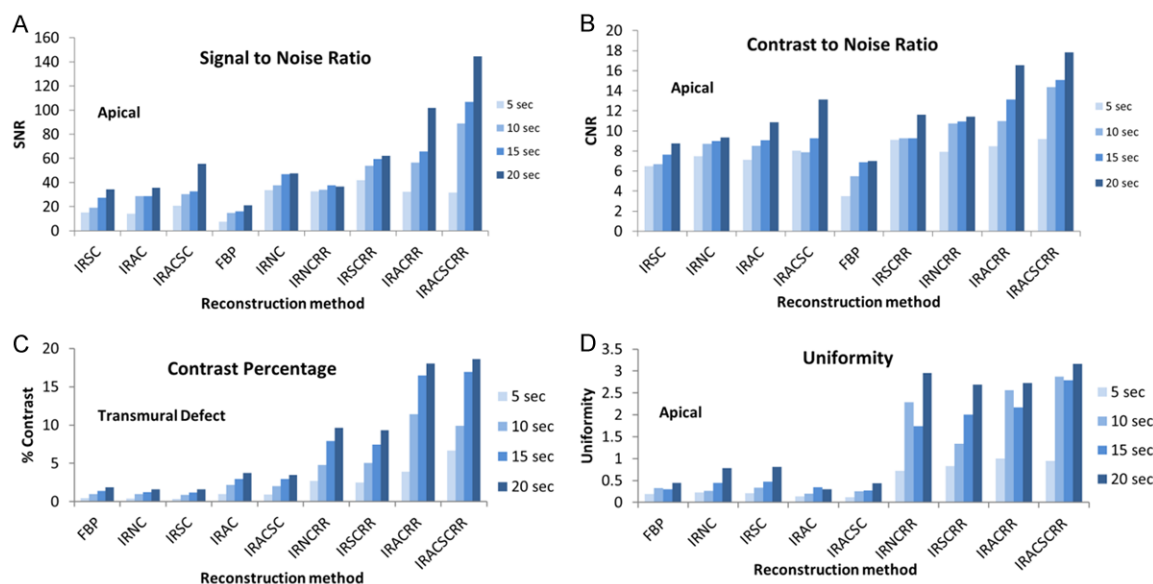


Figure 3. The impact of different count density/projection is showing slight increase in image non-uniformity as longer time is applied. (A) SNR, (B) CNR, (C) Defect contrast percentage. The improvement was in the direction of applying more corrections; however, shorter acquisition time shows percentage improvement 315%, 163% and 1426% respectively. (D) Image uniformity shows negligible increase in image non-uniformity as measured 1.17 at apical slices and 0.7 at basal part.

of iterations and subset used. With respect to defect contrast, the IRAC was comparable to IRACSC and both were higher than IRSC. The improvement was more remarkable for transmural and non-transmural defects such that the best improvement obtained for apical slices was 290%, 161%, and 65% respectively. Interestingly, those improvements were obtained at the same number of iterations and subsets (20 iterations and 12 subsets).

When RR was employed in the iterative reconstruction, the defect contrast significantly improved reporting 901%, 869%, 402%, and 416% for IRACSCRR, IRACRR, IRSCRR and IRNCRR respectively.

When different acquisition times were applied CNR, SNR and defect contrast showed an improvement with increasing time/projection is applied. The time reduction down to 5 sec/projection for IRACSCRR showed an improvement in CNR and SNR without a compromise in image quality. The percentage improvement was 315% and 163% for SNR and CNR respectively for apical slices. Defect contrast percentage improvement was of 1426% and 976% for transmural versus non-transmural defect. Despite this improvement adding more correc-

tions was associated with a negligible increase in noise level as reported by measurements of uniformity and CoV, reaching maximum at basal slices (1.17 and 0.7 respectively) of full time FBP as demonstrated in **Figure 3**.

The angular sampling and total number of views per acquisition showed an impact on image quality as shown from figures of merit analysis. As compared to standard angular increment using FBP, CNR showed an improvement in apical slices being less as we move towards the basal portion of the myocardium. Although the percentage improvement showed enhancement of IR-RR, this percentage decreased as angular increment was reduced (i.e. 9°, 6°, 3° and 2°), but was still superior to FBP. The improvement percentage measured in this direction was 99%, 64%, 37% and 11% respectively for IR-RR full corrections applied.

Furthermore, IR with full corrections showed enhanced performance in the direction of reducing the angular step for apical slices as compared to FBP; the improvement of SNR was very limited in basal slices. The improvement percentage was 162% versus 53% for apical and basal slices respectively. The improvement in cold defect contrast was in favor

SPECT MP image quality with OSEM-RR

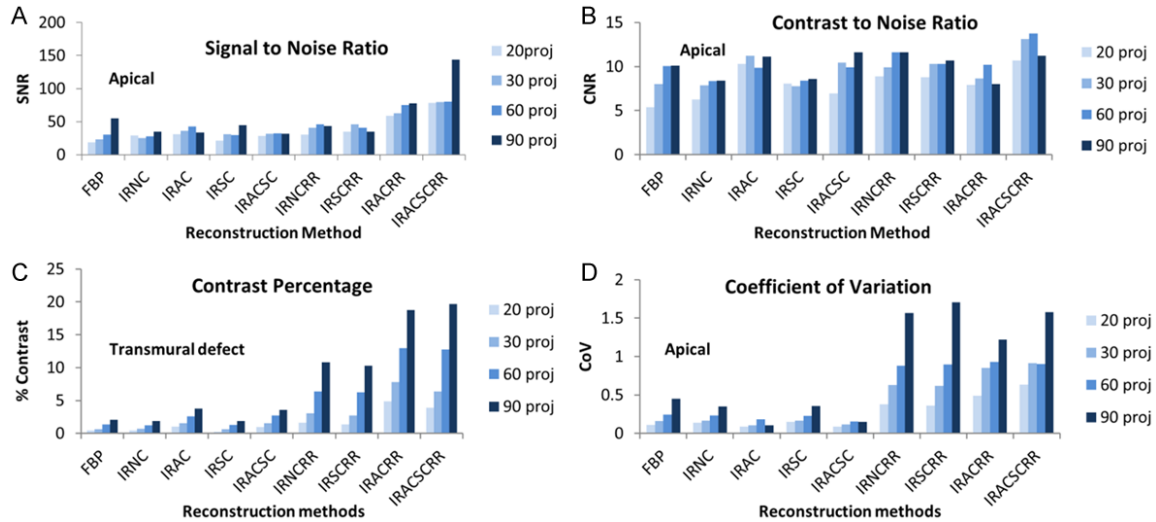


Figure 4. Figures of merit showing the impact of angular sampling on image quality of MPI. (A) SNR as shown there was remarkable improvement in the direction of reducing angular sampling and as more corrections were applied. The highest percentage improvement recorded for IRACSCRR at 2° was 162%. (B) CNR there is a gradual improvement in the image contrast as the number of views is increased (C) Defect contrast percentage. Full corrections IR-RR showed enhanced performance in the direction of decreasing the angular sampling for both type of defects. The percentage improvement was 850% defect with respect to FBP for angular sampling of 2°. (D) Coefficient of variation shows slight increase in the direction of elevating angular sampling and applying more corrections. However, this increase is not significantly high (i.e. not more than 2.50% at maximum).

Table 3. Summary of proposed protocol results for myocardial perfusion SPECT imaging for apical versus basal slices and transmural versus non-transmural defects

	IRACSCRR (5 sec/projection)	
	Apical slices	Basal slices
CNR	1.30 fold	1.20 fold
SNR	2.50 fold	2.20 fold
Uniformity	0.80 fold	1.20 fold
CoV	0.30 fold	0.36 fold
Defect Contrast	8.00 fold	4.08 fold

Results shown with respect to full time standard protocol 20 sec/projection of FBP reconstruction.

of reducing angular step and in the direction of applying more corrections. This improvement showed the role of AC in improving the defect contrast as shown from percentage improvement for transmural defect; 131%, 129%, 96% and 82% versus 116%, 135%, 103% and 71% for AC and ACSC respectively. Furthermore, this improvement was also documented as AC was combined with RR and it was 805% and 850% for IRACRR and IRACSCRR respectively at 90 projections. A typical trend of image non-uniformity and noise was observed as for other tested parameters, **Figure 4** shows figures of merit for number of projections.

Standard versus proposed protocol

The results showed better performance of acquisition/reconstruction parameters of the proposed protocol (5 sec/projection, 90 projections) against standard parameters (20 sec/projection, 60 projections) for CNR, SNR and defect contrast. However, standard protocol showed a minimal change in image noise represented by image uniformity and coefficient of variation. The difference was 0.80 and 0.30 fold for uniformity and CoV respectively with respect to proposed parameters in apical slices versus 1.20 and 0.36 in basal slices. The difference in these terms is considered non-significant and has no impact on the image quality. IRACSCRR provides higher performance in terms of CNR, SNR and defect contrast percentage as shown in **Table 3**. The improvement was 1.3, 2.5 and 8 fold respectively over standard FBP. **Figure 5** shows the potential of time reduction of IRACSCRR versus standard FBP whereas **Figure 6** demonstrates the relative merits attained when different reconstructions and image corrections are applied.

Discussion

Evolution software as a reconstruction algorithm for MPI has been designed by a combina-

SPECT MP image quality with OSEM-RR

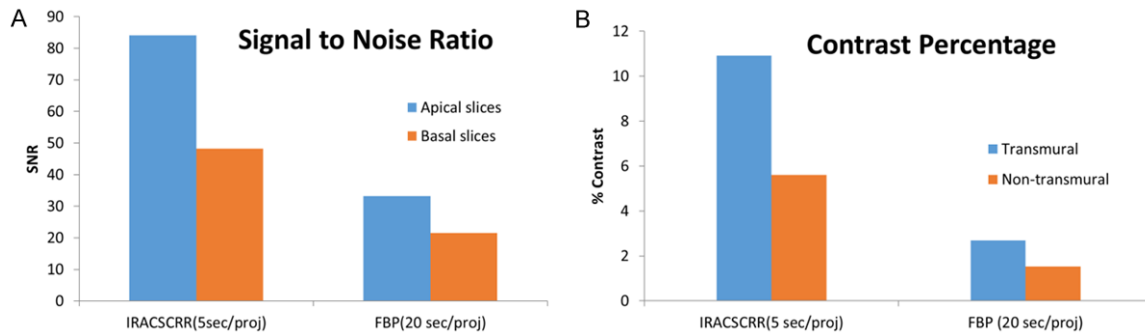


Figure 5. Image quality evaluated for 5 sec/projection OSEM-RR and full time (20 sec/projection) FBP. OSEM-RR with total acquisition time reduction by 63% of full time analytical method shown improved the image quality as seen from figures of merit. A. Signal to noise ratio, OSEM-RR showed remarkable improvement of 2.50 fold and 2.20 fold of full time FBP for apical and basal slices respectively. Although the improvement was observed for apical and basal slices but it is more remarkable for apical portion the improvement percent was 153.20% versus 80.30% in basal part. B. Defect contrast percentage displayed significant enhancement of OSEM-RR algorithm versus conventional method the improvement was of 8 and 4.08 folds of FBP for transmural and non-transmural defects respectively. Standard versus proposed protocol.

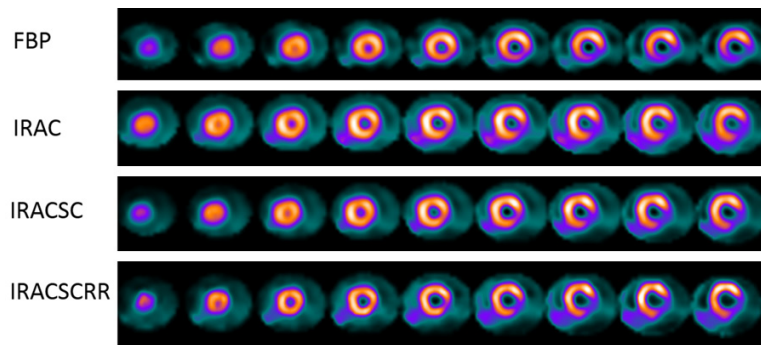


Figure 6. Myocardial perfusion SPECT images reconstructed using the conventional analytic FBP, iterative reconstruction combined with scatter correction (IRSC), iterative reconstruction with attenuation and scatter correction (IACSC) and finally iterative reconstruction with full corrections including attenuation and scatter combined with resolution recovery (IRACSCRR). Attenuation correction appears to restore counts in different segments of the myocardium while scatter correction tends to reduce noise levels with improvement of cavity contrast. When these corrections are combined with resolution recovery there is remarkable improvement in defect as well as left ventricle cavity contrast, more sharpening of myocardial boundaries and overall image quality.

tion of an OSEM iterative reconstruction algorithm and modeling methods to accurately compensate for the image degrading factors [19]. Patient attenuation and scatter either generated within patient or collimator scatter were well modeled and resolved in Evolution™. However, CDR compensation was not completely implemented [13, 20]. Full implementation of CDR is demanding in terms of computation cost and hence geometric compensation is the only correction applied to clinical applications [14].

The results presented in this work showed the effectiveness of iterative reconstruction algorithm with resolution recovery relative to conventional filtered back projection. Iterative reconstruction is able to improve image quality especially when resolution recovery is applied. Scatter, attenuation and detectors response are image degrading factors that are not considered by analytical methods and therefore analytical reconstructions exhibit poor image quality. On the other hand, iterative reconstruction with detector response, attenuation and scatter corrections does account for those degrading factors which subsequently

impact diagnostic performance to a greater extent [14, 21, 22]. There was a gradual improvement as more corrections were applied.

With regard to the numbers of iterations and subsets, it was shown that the improvement was more remarkable as resolution recovery correction was applied to iterative reconstruction. The implementation of resolution recovery in the IR algorithm is more effective than changing the iteration/subset number. This added value of RR over iteration/subset number is

because resolution recovery compensates for the detector-patient distance considering the detector response function [13, 14]. However; with iteration/subset number no additional corrections are applied but generating a new estimate to reach the predefined condition to approach the image.

In terms of different acquisition times, the strength of IR-RR is obviously superior to either FBP or IR without RR correction. IR-RR was able to preserve acceptable image quality with time reduction down to one fourth of standard time/projection or one-third of total time of that for FBP. CDR compensation is valuable and effective to compensate the time reduction which in-turn affect the count density but without compromising the image quality [21].

The impact of angular increment on image quality was evaluated and results of IR-RR showed that resolution recovery could adapt to faster increment (9°) as well as slower increment (2°) with improved image quality in the direction towards the slow angular increment.

Considering these results, a new imaging protocol was proposed and evaluated versus the standard protocol in terms of acquisition and reconstruction parameters. Although there was a time reduction down to one third of full time FBP, iterative reconstruction with CDR compensation provided myocardial image quality equivalent to that yielded by full-time FBP. Moreover, iterative reconstruction with resolution recovery is more effective at the apical slices with reduced performance in basal portion of myocardium. This was observed in many instances of this study which requires further attention during the interpretation of myocardial perfusion images and needs to be addressed by software developers.

Compared to FBP, Evolution[®] with different combination of corrections showed very minimal increase in noise. The elevated level of noise associated with OSEM-RR could have several explanations. Among those, the number of iterations required to achieve the convergence is high as CDR compensation is applied [20]. Furthermore, OSEM as iterative statistical reconstruction method is associated with high level of noise. The tradeoff between number of iterations and smoothing function may improve the noise texture. Moreover, the noise level could increase most probably due to noise

amplification during scatter correction step. Note that the scatter correction applied was a dual window-based technique which relatively serves to boost the noise level in the reconstructed images [12, 15].

OESM-RR showed high performance in terms of defect contrast when compared to FBP and OSEM without RR. In this context several clinical studies conclude that iterative reconstruction compensating for CDR improves defect detection. In addition, the role of regularization plays an important role in improving this performance [20].

The results presented here are not easily translatable to another imaging system and/or iterative reconstruction algorithms as every vendor has its own implementation specifics related to scanner performance, detector response, reconstruction parameters, regularizations and convergence rates. However, the results obtained are in good agreement with previous approaches and reconstruction methods [21, 23].

There were some limitations associated with the study which is not consistent in part with real clinical practice. First, the cardiac insert was located in the cylindrical symmetrical Jaszack phantom, and therefore the data might bear some underestimation of the amount of photon attenuation observed in average human. Second, the static cardiac phantom used in the study didn't permit one to perform gated MPI and thus quantitative analysis of left ventricular functional parameters like ejection fraction, end systolic, end diastolic and stroke volumes couldn't be evaluated. Third, the left ventricular background used has not considered wide range of background activities that might be seen in liver or lung tissues. However, a reasonable average was used in the study to mitigate the influence background heterogeneity.

Therefore, future studies are warranted to pursue this work with dynamic cardiac phantoms, more variable and realistic background activities along with true clinical studies in comparison to gold standards methods of coronary artery disease.

Conclusion

Evolution software provides clinically acceptable image quality for shorter acquisition time

compared to that for FBP of image reconstruction. Hence, acquisition time reduction down to one third of the standard acquisition time may be applied with no impact on myocardium perfusion image quality and clinical findings.

Compared to analytical algorithm, IRR (Evolution) provide image quality with high performance in MPI studies in terms of SNR, CNR and defect contrast. Although the post reconstruction filter recommended by the manufacturer was applied, there is still room for further improvement by proper selection of the cut-off frequency and filter order. This could help to some extent in reducing some residual noise retained in image reconstruction while providing further enhancement of image quality.

Optimal performance requires proper regularization by post filtering. Accordingly, optimization of potential factors including proper selection of iteration/subset number, post filtering and smoothing function and its cutoff frequency may reduce image noise. Moreover, IR-RR showed a lower performance for basal myocardium slices when compared to the apical portion of the myocardium. This observation is of particular importance to reading physicians and would be a matter of future investigations in our laboratory.

The reduction of acquisition time was found applicable but its immediate use in all patient studies needs further investigation especially when combined within the framework of attenuation and scatter correction. This study provides additional evidence that full correction scheme with reduced imaging time is yielding better improvement in image quality of MPI compared to FBP reconstruction. Additional practical benefits of these findings can be a reduction of the administered radioactivity and hence less radiation exposure to patients as well as nuclear medicine staff members and increased patient throughput in busy nuclear cardiology laboratories.

The proposed protocol in this study which included 90 projections, 5 sec/projection and IR-RR with full corrections (i.e. IRACSCRR) was shown superior to the standard protocol provided by system manufacturer. The main benefit is time reduction providing one fourth of standard projection time (i.e. one third of total acquisition time) in terms of CNR, SNR and

defect contrast while maintaining a reasonable noise level. Therefore, the future aim is to validate that protocol in clinical studies in comparison to the reference methods of coronary artery disease.

Disclosure of conflict of interest

None.

Address correspondence to: Dr. Magdy M Khalil, Department of Physics, Faculty of Science, Helwan University, Cairo, Egypt. E-mail: magdy_khalil@hotmail.com

References

- [1] Berman DS, Shaw LJ, Min JK, Hachamovitch R, Abidov A, Germano G, Hayes SW, Friedman JD, Thomson LE, Kang X, Slomka P and Rozanski A. SPECT/PET myocardial perfusion imaging versus coronary CT angiography in patients with known or suspected CAD. *J Nucl Med Mol Imaging* 2010; 54: 177-200.
- [2] Hachamovitch R, Berman DS, Shaw LJ, Kiat H, Cohen I, Cabico JA, Friedman J and Diamond GA. Incremental prognostic value of myocardial perfusion single photon emission computed tomography for the prediction of cardiac death: differential stratification for risk of cardiac death and myocardial infarction. *Circulation* 1998; 97: 535-543.
- [3] Gimelli A, Rossi G, Landi P, Marzullo P, Iervasi G, L'abbate A and Rovai D. Stress/rest myocardial perfusion abnormalities by gated SPECT: still the best predictor of cardiac events in stable ischemic heart disease. *J Nucl Med* 2009; 50: 546-553.
- [4] Galassi AR, Azzarelli S, Tomaselli A, Giosofatto R, Ragusa A, Musumeci S, Tamburino C and Giuffrida G. Incremental prognostic value of technetium-99m tetrofosmin exercise myocardial perfusion imaging for predicting outcomes in patients with suspected or known coronary artery disease. *Am J Cardiol* 2001; 88: 101-106.
- [5] DePuey EG. Advances in SPECT camera software and hardware: currently available and new on the horizon. *J Nucl Cardiol* 2012; 34: 1071-3581.
- [6] Mangla A, Oliveros E, Williams KA Sr and Kalra DK. Cardiac imaging modalities in the diagnosis of coronary artery disease. *Curr Probl Cardiol* 2017; 42: 316-366.
- [7] Tonge CM, Manoharan M, Lawson RS, Shields RA and Prescott MC. Attenuation correction of myocardial SPECT studies using low resolution computed tomography images. *Nucl Med Commun* 2005; 26: 231-237.

- [8] Koepfli P, Hany TF, Wyss CA, Namdar M, Burger C, Konstantinidis AV, Berthold T, Von Schulthess GK and Kaufmann PA. CT attenuation correction for myocardial perfusion quantification using a PET/CT hybrid scanner. *J Nucl Med* 2004; 45: 537-542.
- [9] O'Connor MK and Kemp BJ. Single-photon emission computed tomography/computed tomography: basic instrumentation and innovations. *Semin Nucl Med* 2006; 36: 258-266.
- [10] Khalil M. *Basic Sciences of Nuclear Medicine*, Springer Verlag Heidelberg Dordrecht London New York. 2011.
- [11] Chun SY, Fessler JA and Dewaraja YK. Correction for collimator-detector response in SPECT using spread function template. *Med Imaging* 2013; 32: 295-305.
- [12] Zaidi H and Koral KF. Scatter correction strategies in emission tomography. In *Quantitative Analysis in Nuclear Medicine Imaging* H. Zaidi (edition). Springer: New York; 2005. pp. 205-230.
- [13] Ghaly M, Links JM and Frey EC. Collimator optimization and collimator-detector response compensation in myocardial perfusion SPECT using the ideal observer with and without model mismatch and an anthropomorphic model observer. *Phys Med Biol* 2016; 61: 2109-2123.
- [14] Naum A, Kleven-Madsen N, Biermann M, Johnsen B, Tvedt BA, Rotevatn S, et al. Quantitative comparison of myocardial perfusion defects using different reconstruction algorithms. *J Clinic Experiment Cardiol* 2011.
- [15] In: Cherry SR, Sorenson JA and Phelps ME, editors. *Physics in Nuclear Medicine*. 4th edition, Philadelphia: WB. Saunders; 2012.
- [16] Narayanan MV, King MA, Pretorius PH, Dahlberg ST, Spencer F, Simon E, Ewald E, Healy E, MacNaught K and Leppo JA. Human-observer receiver-operating-characteristic evaluation of attenuation, scatter, and resolution compensation strategies for ^{99m}Tc myocardial perfusion imaging. *J Nucl Med* 2003; 44: 1725-1734.
- [17] Slomka Piotr, et al. "Digital/fast SPECT: systems and software". *Clinical Nuclear Cardiology*. 4th edition. Philadelphia: Elsevier Mosby; 2010. pp. 132-48.
- [18] DePuey EG, Gadiraju R, Clark J, Thompson L, Anstett F and Shwartz SC. Ordered subset expectation maximization and wide beam reconstruction "half-time" gated myocardial perfusion SPECT functional imaging: a comparison to "full-time" filtered back projection. *J Nucl Cardiol* 2008; 15: 547-563.
- [19] Slomka PJ, Patton JA, Berman DS and Germano G. Advances in technical aspects of myocardial perfusion SPECT imaging. *J Nucl Cardiol* 2009; 16: 255-76.
- [20] Frey EC and Tsui BMW. Collimator-Detector response compensation in SPECT. In *quantitative analysis in nuclear medicine imaging*. In: Zaidi H, editor. Springer: New York; 2005. pp. 141-161.
- [21] Zoccarato O, Scabbio C, De Ponti E, Matheoud R, Leva L, Morzenti S, Menzaghi M, Campini R, Marcassa C, Del Sole A, Garancini S, Crivellaro C, Brambilla M and Lecchi M. Comparative analysis of iterative reconstruction algorithms with resolution recovery for cardiac SPECT studies. A multi-center phantom study. *J Nucl Cardiol* 2014; 21: 135-148.
- [22] Marcassa C and Zoccarato O. Advances in image reconstruction software in nuclear cardiology: is all that glitters gold? *J Nucl Cardiol* 2017; 24: 142-4.
- [23] Brambilla M, Lecchi M, Matheoud R, Leva L, Lucignani G, Marcassa C and Zoccarato O. Comparative analysis of iterative reconstruction algorithms with resolution recovery and new solid state cameras dedicated to myocardial perfusion imaging. *Phys Med* 2017; 41: 109-116.